Nat Hazards
DOI 10.1007/s11069-015-1640-y

ORIGINAL PAPER

Coupled fire–atmosphere modeling of wildland fire spread using DEVS-FIRE and ARPS

Nathan Dahl · Haidong Xue · Xiaolin Hu · Ming Xue

Received: 3 November 2014 / Accepted: 28 January 2015
© US Government 2015

Abstract This article introduces a new wildland fire spread prediction system consisting of the raster-based Discrete Event System Specification Fire model (DEVS-FIRE) and the Advanced Regional Prediction System atmospheric model (ARPS). Fire–atmosphere feedbacks are represented by transferring heat from DEVS-FIRE to ARPS as an externally forced set of surface fluxes and mapping the resulting changes in near-surface wind from ARPS to DEVS-FIRE. A preliminary evaluation of the performance of this coupled model is performed through idealized tests and an examination of the September 2000 Moore Branch Fire; the results conform well with those of other coupled models and are superior to those produced by the uncoupled DEVS-FIRE model, motivating further investigation.

Keywords Discrete event specification · Moore Branch Fire

1 Introduction

Accurate prediction of wildland fire behavior is essential for ensuring firefighter safety and optimizing firefighting resource management during outbreaks. Various fire spread models have been developed (e.g., the FARSITE model described in Finney 1998). However, many operational models neglect the possibility of substantial feedbacks between the fire

N. Dahl (✉)
Rosenstiel School of Marine and Atmospheric Science, University of Miami, 4600 Rickenbacker Causeway, Miami, FL 33149, USA
e-mail: ndahl@rsmas.miami.edu

H. Xue · X. Hu
Department of Computer Science, Georgia State University, P.O. Box 5060, Atlanta, GA 30302, USA

M. Xue
Center for Analysis and Prediction of Storms, 120 David L. Boren Boulevard, Suite 2500, Norman, OK 73072, USA

Published online: 08 February 2015

and the atmosphere above it. As discussed in Clark et al. (1996), heat from the fire produces buoyancy gradients in the atmosphere and consequent modification of near-surface winds, which can locally increase the rate of fire spread and attendant heat release into the lower atmosphere. The degree of coupling varies widely, from "wind-driven" fire spread dominated by the background atmosphere to "plume-driven" fire spread dominated by the heat released by the fire (Byram 1959). However, significant coupling is not always observed even in cases where it is theoretically predicted (Sullivan 2007); clearly, a full understanding of the factors influencing wildland fire behavior remains elusive.

Accounting for fire–atmosphere feedbacks through coupled numerical simulations is a relatively novel concept and generally involves an atmospheric model and a fire spread model running in parallel. In this approach, the near-surface conditions from the atmospheric model are fed into the fire model at spatial and temporal resolutions much greater than those available from general weather observations, while the heat output from the simulated fire is fed into the lower levels of the atmospheric model. A variety of approaches are used to represent the heat output in the weather model. For example, CAWFE (Clark et al. 2004) and WRF-FIRE (Mandel et al. 2011) calculate heat fluxes from combustion rates (determined from an exponential decay function) and distribute the sensible heat flux vertically to account for radiation, while MesoNH/ForeFire (Filippi et al. 2011) uses "nominal" values based on fuel type to estimate the heat fluxes and effective emitting temperature in order to treat radiation explicitly. Likewise, there are different ways of representing flame front spread (rate and direction) in wildland fire models. CAWFE and MesoNH/ForeFire treat the front as an expanding polygon with spread rates determined from semi-empirical functions such as those derived by Rothermel (1972). WRF-FIRE uses a level-set method (also based on the Rothermel functions) interpolated across multiple cells to assess the position of the fire front as well as the burn time and fuel consumption at each cell within the burn area. A third approach is to use a "raster-based" method to treat the fire spread as a series of cell-to-cell interactions rather than the propagation of a contiguous front. Different proposed cell interaction rules have motivated the development of a variety of raster-based fire simulation models (e.g., Kourtz and O'Regan 1971; Green et al. 1983; Vasconcelos and Guertin 1992; Karafyllidis and Thanailakis 1997; Lopes et al. 2002; Achtemeier 2003; Peterson et al. 2009; Trunfio et al. 2011).

Although the raster-based approach is widely used in uncoupled modeling, its utility in coupled fire–atmosphere modeling has not been intensively investigated. Achtemeier (2013) performed a limited validation of a coupled framework using a cellular automata (CA; see von Neumann 1966) fire spread model based on "Rabbit Rules" and noted a vast improvement in computational speed compared with the capabilities of HIGRAD/FIRETEC, but that validation was limited to the response within the surface layer over a time frame of several minutes; furthermore, the use of "Rabbit Rules" and a simple interface weather model in those tests prevented Achtemeier's model from simulating four-dimensional interactions between the fire plume and the ambient environment. This article presents an effort to develop coupled fire–atmosphere modeling with a raster-based fire spread model called DEVS-FIRE (Ntaimo et al. 2004, 2008; Hu et al. 2012). DEVS-FIRE is a discrete event simulation model that also supports fire suppression simulation with realistic tactics (e.g., direct attack, parallel attack, and indirect attack) and has been integrated with a stochastic optimization model to guide the allocation of firefighting resources (Hu and Sun 2007; Hu and Ntaimo 2009). Furthermore, dynamic data assimilation methods have recently been implemented which improved DEVS-FIRE simulation results significantly (Xue and Hu 2011; Xue et al. 2012a, b).

The original DEVS-FIRE model treats weather as an external input and therefore does not account for coupled fire–atmosphere feedbacks. Since accurate depiction of fire spread is essential for determining an optimal firefighting response, a coupled model consisting of DEVS-FIRE and the Advanced Regional Prediction System (ARPS; Xue et al. 2000, 2001) atmospheric model is introduced here. The ARPS model was initially designed to simulate intense small-scale atmospheric convection but has been equipped with the formulations and parameterizations necessary to operate at a wide range of scales, including the scales at which fire–atmosphere feedbacks become significant. This article will proceed by briefly describing DEVS-FIRE and ARPS individually, outlining the method by which they are coupled, and providing a preliminary evaluation of the performance of the coupled model through a series of idealized tests and an examination of the September 2000 Moore Branch Fire. Plans for further investigation will then be summarized in light of the results.

2 Component models

2.1 DEVS-FIRE

As classified in Sullivan (2009), the DEVS-FIRE model is a CA-based fire spread and suppression simulation model. DEVS-FIRE is constructed and described by the Discrete Event System Specification (Zeigler et al. 2000). It has a raster-based fire representation in which the fire space is divided into contiguous cells and the propagation algorithm is based on cell interactions (i.e., the direct-contact-based perimeter expansion). After a cell is ignited, the Rothermel model (1972) is employed to calculate fire spread rates toward all neighboring cells. When a fire spreads to a cell border, a message is sent to ignite the corresponding adjacent cell. A discrete event simulation engine manages all cell behavior, and then, the overall fire propagation is simulated, with integrated fire suppression (Hu et al. 2012) and dynamic-data-driven simulation (Xue et al. 2012a, b) supported as needed.

2.1.1 Fire spread

In DEVS-FIRE, a fire area is modeled as a set of rectangular cells. Different cells may have different fuel types, terrain information, and weather conditions according to the spatial geographic information system (GIS) data and weather data (which typically change dynamically over time). However, within each cell, the fuel, terrain, and weather data are assumed to be spatially constant. Table 1 lists the input cell variables, which mostly correspond to the inputs of the Rothermel model.

Fire spread is modeled as a propagation process as burning cells ignite their immediate neighbors. Once a cell is ignited, the maximum spread direction and the spread rate in that direction are first computed from the wind and slope based on the Rothermel model (see Sharples 2008 for a review of different methods for wind-slope correction of fire spread rate). Similar to the method in Finney (1998), the spread rate in the maximum spread direction is then decomposed according to an elliptical shape, from which the spread rates toward the cell's eight neighbors are calculated as illustrated in Fig. 1. Based on the spread rates and distances to the centers of the corresponding neighboring cells, the time to ignite those cells is scheduled. This cellular approach naturally accounts for inhomogeneity in the slope and composition of the fuel bed, and the uncoupled DEVS-FIRE output has been validated through comparison with fire spread simulation results from FARSITE under a variety of conditions (Gu et al. 2008). Furthermore, the discrete event specification and

Table 1 DEVS-FIRE cell input variables

Variable	Unit
Oven-dry fuel loading[a]	kg/m^2
Fuel depth[a]	m
Fuel particle surface area-to-volume ratio[a]	1/m
Fuel particle low heat content[a]	kJ/kg
Oven-dry particle density[a]	kg/m^3
Fuel particle moisture content[a]	1
Fuel particle total mineral content[a]	1
Fuel particle effective mineral content[a]	1
Wind velocity at mid-flame height[a]	m/s
Wind direction[a]	degree
Vertical rise/horizontal distance (slope)[a]	degree
Slope direction	degree
Moisture content of extinction[a]	1
x dimension	m
y dimension	m

[a] Inputs of the Rothermel model

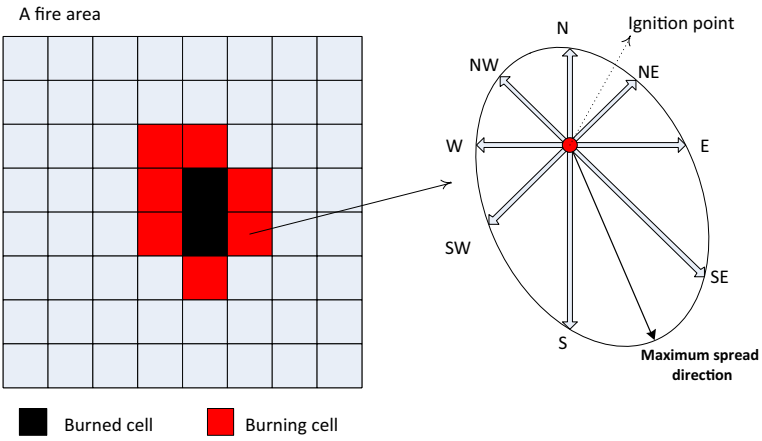

Fig. 1 Fire spread decomposition in DEVS-FIRE

raster-based approach employed in DEVS-FIRE have a greater potential for computational efficiency than the time integration (with an inherent limit on time step size in order to maintain stability and realism) and vector-based approach employed in models like FARSITE.

2.1.2 Heat generation

The heat generated from the Rothermel model does not apply to non-fire-front fire areas, so DEVS-FIRE implements a separated post-frontal combustion heat model that computes the heat flux for the non-fire-front areas (Xue et al. 2012a, b). For each ignited cell, DEVS-FIRE first calculates the total burning time using the BURNUP model (Albini and

Reinhardt 1995). Similar to the method in WRF-FIRE (Mandel et al. 2011), the fractional unburned fuel mass remaining is modeled as an exponentially decreasing function before the burning time in BURNUP is reached. After that, the fuel mass decrease stops. The fuel mass fraction function is as follows:

$$F(t) = \begin{cases} \exp\left(-\dfrac{t}{C\tau_c}\right), & t \le \tau_c \\ \exp\left(-\dfrac{1}{C}\right), & t > \tau_c \end{cases} \quad \text{where} \quad \tau_c = \frac{T'_F - T'_C}{T_F - T_C}\frac{\rho_0}{\rho'_o}\frac{D(0)}{h_{eff}}(a' + b'M), \tag{1}$$

τ_c is the burning time (specified for the given fuel type), $D(0)$ is the initial fuel diameter, h_{eff} is the heat transfer coefficient (W m^{-2} K^{-1}), T_F is the temperature of fire (K), T_C is the sublimation temperature (K), ρ_o is the oven-dry fuel mass density (kg m^{-3}), M is the fuel moisture fraction by mass (dimensionless), and T'_F (K), T'_C (K), ρ'_o (kg m^{-3}), a′ (J m^{-3} K^{-1}), and b′ (J m^{-3} K^{-1}) are scale values determined by BURNUP experiments. Where the expected final fuel fraction at time τ_c is known, this equation is used in advance to solve for the dimensionless parameter C for the given fuel type, which is then used for all calculations after ignition at that location. Wind speed influences the reduction rate via h_{eff}, which consists of a convective heat transfer coefficient (determined in part by the winds) and a radiative transfer coefficient. After the fuel fraction loss $F(t) - F(t + \Delta t)$ is computed over a time period Δt, the sensible and latent heat fluxes from the fire are modeled using the total heat density from the Rothermel model as:

$$\phi_h = \frac{(F(t) - F(t + \Delta t))}{\Delta t}\frac{1}{1 + M}w_\eta h, \tag{2}$$

$$\phi_q = \frac{(F(t) - F(t + \Delta t))}{\Delta t}\frac{0.56 + M}{1 + M}w_\eta L, \tag{3}$$

where ϕ_h is the sensible heat flux, ϕ_q is the latent heat flux, w_n is the net fuel load, M is the fractional fuel moisture content by mass, w_η is the mineral damping coefficient, h is the fuel particle low heat content, and L is the latent heat of evaporation for water.

For a given fuel type, popular heat flux models (e.g., the one in Mandel et al. 2011) employ a static fuel loss curve. As a result, certain pertinent environmental factors (e.g., the impact of stronger winds on combustion rate/efficiency at a given location) are not addressed when calculating the fuel loss rate and associated fluxes. More accurate burn rate and heat flux calculations are sought in the DEVS-FIRE heat flux model (i.e., the one in Xue et al. 2012a, b) by introducing empirical estimates of those factors as indicated by (1). However, when the two coefficients a' and b' in (1) are not available (as in the experiments presented here), DEVS-FIRE still employs the static fuel loss curve model as in Mandel et al. (2011), which describes the fuel mass fraction as:

$$F(t) = \exp(-t/T_f), \tag{4}$$

$$T_f = \frac{W}{0.8514}, \tag{5}$$

where T_f is the number of seconds for a fuel to burn down to $1/e \approx 0.3689$ of the original quantity and W is an empirically determined weighting factor (Clark et al. 2004). For each fuel type, W determines the fuel mass loss curve.

Using (2) and (3), given a time period, the time-averaged surface heat fluxes for an ignited cell can be calculated. Figure 2 displays an example DEVS-FIRE simulated fire

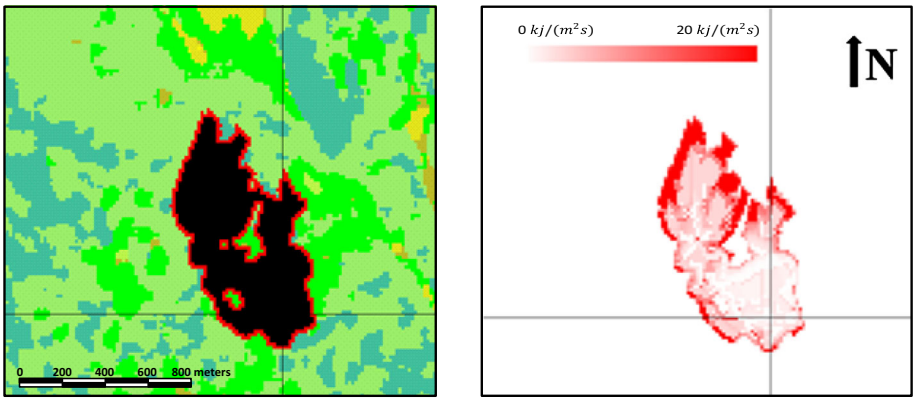

(a) Fire front **(b)** Heat flux

Fig. 2 An example of (*left*) an uncoupled DEVS-FIRE front and (*right*) its corresponding heat flux in the preceding 10 min in a heterogeneous fuel bed. In the *left panel*, the fire front position is marked in *red*, other ignited (burning or burned out) cells are in *black*, and the remaining colors illustrate fuel type (*yellow* for short grass, *brown* for logging slash, *bright green* for timber litter, *drab green* for southern rough, and *turquoise* for hardwood litter)

and its corresponding heat flux. In Fig. 2a, the red cells are the fire front and the black cells are in the non-fire-front area. Figure 2b shows that a reasonable magnitude for the time-averaged heat flux is generated (see observed values in Clements et al. 2007), and ARPS is employed in this study to capture the impact of such heat fluxes on the weather.

2.2 ARPS

ARPS is a three-dimensional numerical weather prediction model developed by the Center for Analysis and Prediction of Storms. A detailed description of its formulation and features is beyond the scope of this paper, and the reader is referred to Xue et al. (2000, 2001). However, characteristics related to its coupling with DEVS-FIRE are summarized here. First, while ARPS contains formulations of the atmospheric governing equation that are appropriate at a wide range of scales, it was initially developed for the purpose of modeling intense, small-scale convective phenomena. This primary focus makes ARPS readily adaptable to the task of modeling the rapid, localized shifts in the atmospheric mass and wind fields that a wildland fire might produce.

Similar to other atmospheric models (e.g., WRF; Skamarock et al. 2008), ARPS operates on a transformed coordinate system that accounts for the local terrain. Through hyperbolic grid stretching, the model domain follows the terrain at low levels and gradually approaches a constant-altitude plane aloft. Grid stretching enables more high-resolution treatment of turbulent boundary layer processes while retaining (at comparatively low cost) a sufficiently deep computational domain to contain the more intense plumes that can develop; for example, in the simulations detailed in this study, it was feasible to extend the ARPS domain to an altitude of several kilometers while operating at near-surface vertical resolutions on the order of a few meters (Numerical stability was maintained in these cases by using a vertically implicit scheme to handle fast wave modes and turbulent mixing).

The terrain-following transformation may also be beneficial for fire spread modeling in moderately varied terrain where the component of the wind responsible for spreading the fire is not purely horizontal. Using North America geological survey data available at horizontal resolutions ranging from $\sim$20 km down to 100 m or less, ARPS is able to map terrain variations at scales corresponding to wildland fires. It is noted that the use of terrain-following coordinates is a significant source of error in highly complex (e.g., urban) or very steep terrain, particularly when the horizontal resolution is much coarser than the vertical resolution; this has motivated the development of alternative treatments of the interaction between terrain and the lower boundary of the atmospheric model (e.g., the implementation of an "immersed lower boundary" in WRF as detailed in Lundquist et al. 2012). However, along with model validation against observational data at coarser resolutions (described in Xue et al. 2000), high-resolution representations of turbulent flows in ARPS have been shown to correspond well to observations over terrain that is much more complex than that used in the experiments shown here (e.g., Chow et al. 2006; Zhou and Chow 2011, 2013, 2014). Therefore, for these preliminary tests, the built-in capabilities of ARPS are suited for coupling with DEVS-FIRE.

3 Description of the coupled model

3.1 Representing fire in ARPS

The uncoupled ARPS model calculates surface heat fluxes with a drag coefficient applied to the temperature difference between the surface and the atmosphere immediately above it (making use of Monin–Obukhov similarity theory; see Obukhov 1946). For typical atmospheric conditions, this is generally effective. However, simply applying this method to the coupled model with the surface temperature replaced by the temperature of ignited fuel is dubious for two reasons. First, the effective temperature of the fire is difficult to estimate reliably when operating at computationally feasible resolutions with heterogeneous fuel beds and rapidly varying atmospheric conditions. Second, there is no guarantee that the assumptions used to obtain the drag coefficients will be valid for the unusual conditions encountered in the vicinity of a fire. For these reasons, the fluxes calculated by DEVS-FIRE (using (2) and (3)) for an ignited region are mapped directly to the corresponding location on the ARPS grid.

When computational cost and time are considered, the constraints placed on the spatial and temporal resolution of the weather model make explicitly modeling turbulent interactions between the fire and the atmosphere at all relevant scales impossible. In keeping with the standard practice of other coupled models (e.g., WRF-FIRE), ARPS/DEVS-FIRE employs a large eddy simulation (LES) approach in which the spatially averaged turbulence characteristics for each ARPS cell are dynamically updated using the 1.5-order subgrid-scale turbulence closure scheme formulated by Moeng (1984). In this scheme, closure is achieved by assuming down-gradient diffusion, with eddy dissipation (as formulated in Kolmogorov 1941) and momentum and heat eddy coefficients (as formulated in Deardorff 1980) all dependent on the subgrid turbulence length scale. In unstable atmospheric stratification (such as would be expected above wildland fires), the estimated length scale is a simple geometric average of the local horizontal and vertical resolutions of the computational grid; therefore, to adequately estimate the vertical distribution of the imposed fluxes and the impact of subgrid-scale momentum transfer, it is still crucial to run ARPS at high spatial resolutions ($\sim$100 m). Furthermore, the model equations are

integrated forward using leapfrog-in-time-centered-in-space discretization with a very small time step specified in ARPS (0.05 s for the idealized tests, 0.1 s for the Moore Branch case) to maintain numerical stability for these experiments.

3.2 Model grid configuration and data mapping

DEVS-FIRE and ARPS operated on separate grids for the simulations in this study, with the DEVS-FIRE domain circumscribed by the ARPS domain. This was done because the boundary conditions used by ARPS may increasingly interfere with the atmospheric response and associated feedbacks if the fire is allowed to spread to the lateral boundaries. Furthermore, intense fire-induced temperature or pressure gradients approaching or intersecting the boundaries can lead to numerical instability and model failure.

Also, identical spatial resolution may not be warranted for both models. On the one hand, operating DEVS-FIRE at a resolution of hundreds of meters results in increasingly discontinuous progression of the fire front, since each instance of fire spread is manifested by discrete ignition of an entire cell; therefore, it is desirable to make the DEVS-FIRE grid resolution as small as the fuel, and terrain data will support (generally $\sim$10 m). On the other hand, reducing the grid spacing in ARPS to such resolutions would limit the integration time step interval to thousandths of a second, which is much too costly to produce a

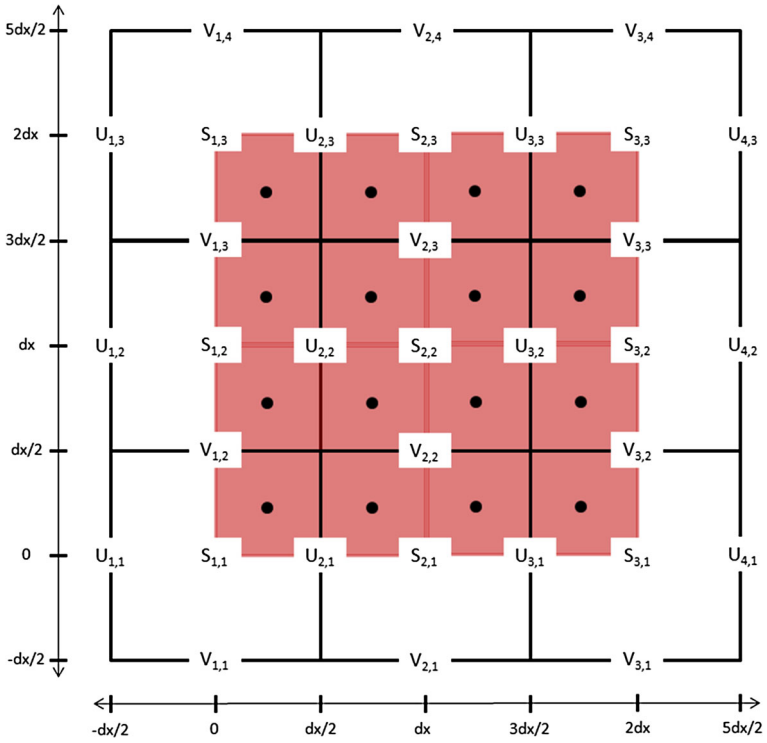

Fig. 3 Model grid map for a 4 × 4 DEVS-FIRE grid of resolution dx/2 centered within a 3 × 3 ARPS domain of resolution dx. Subscripts denote the *x* and *y* indices of the ARPS cells, while each DEVS-FIRE cell is represented as a *pink box* with a *dot* at its *center*

true forecast. Therefore, a weather model grid that is both larger and coarser than the fire model grid seems to be the most reasonable configuration.

ARPS operates on an Arakawa-C grid (Arakawa and Lamb 1977), with vector quantities (e.g., wind components "U" and "V") specified on the faces of each cell and scalar quantities ("S"), such as temperature, specified at the center. Therefore, even when the centers of the ARPS and DEVS-FIRE grids are perfectly collocated as in Fig. 3, it is necessary to interpolate the temperature, humidity, and wind components to estimate the weather conditions for a given DEVS-FIRE cell. To facilitate data exchange between the models, ARPS reads and stores the dimensions and location (specified using the latitude and longitude of the southeast-most cell) of the DEVS-FIRE grid during initialization. An array containing the ARPS x and y coordinates of every cell in the DEVS-FIRE grid is then calculated and stored, providing an inexpensive reference for coordinating the exchange of relevant data between the models.

As discussed previously, explicit representation of microscale turbulent interactions between the atmosphere and the fire is too costly to achieve for a forecast model operating over a domain possibly spanning several kilometers. Sub-grid spatial distributions of mean atmospheric variables such as temperature or wind speed near the fire front are not generally known, and the turbulence characteristics are spatially averaged over the entire grid cell in the LES approach. Therefore, horizontal bilinear interpolation is currently used to map the mean weather conditions from ARPS to the DEVS-FIRE grid (the black dots in Fig. 3), and the influence of subgrid-scale eddies on fire spread rate and direction is estimated based on the interpolated mean wind using the elliptical parameterization described earlier. Similarly, simple spatial averaging is used to map the heat flux output from DEVS-FIRE onto the ARPS grid. For example, with ARPS operating at a horizontal resolution dx, the heat flux from all DEVS-FIRE cells within a distance dx/2 of the scalar location for a fully encompassed ARPS grid cell ("$S_{2,2}$" in Fig. 3) is summed and the result is divided by the total number of DEVS-FIRE cells within that range. Coupled modeling is achieved by repeating this update process throughout the simulation period as detailed below.

3.3 Initialization procedure and time integration algorithm

The general algorithm for integrating the coupled model forward in time is illustrated in Fig. 4. Before running the model, the user obtains the fuel and terrain GIS data and initial fire front position (defined as a set of cell coordinates) for the DEVS-FIRE grid and selects an ARPS domain that fulfills the requirements specified above. The user also selects an update time interval defining the frequency of data exchange between DEVS-FIRE and ARPS. This update time may be adjusted based on computational constraints and the expected time scale of coupled model fluctuations based on spatial resolution; for example, an interval of 60 s was used for the Moore Branch simulations shown below, while smaller intervals may be used for smaller fires modeled at higher resolutions (For further discussion regarding the interval selected for these tests, see Sect. 5).

At initialization, ARPS obtains the wind field (both speed and direction) at 6 m above ground level and maps it to the DEVS-FIRE grid through horizontal interpolation. DEVS-FIRE then ignites the initial fire front, calculates the spread rate from the weather, fuel, and terrain data (using a fuel-type-specific adjustment factor to calculate the midflame wind from the 6 m wind as described in Gu et al. 2008), and moves forward to the next update time. It then calculates the time-averaged heat flux outputs for each cell using (2) and (3) with input from either (1) or (4) and (5) and writes the results back to ARPS. ARPS

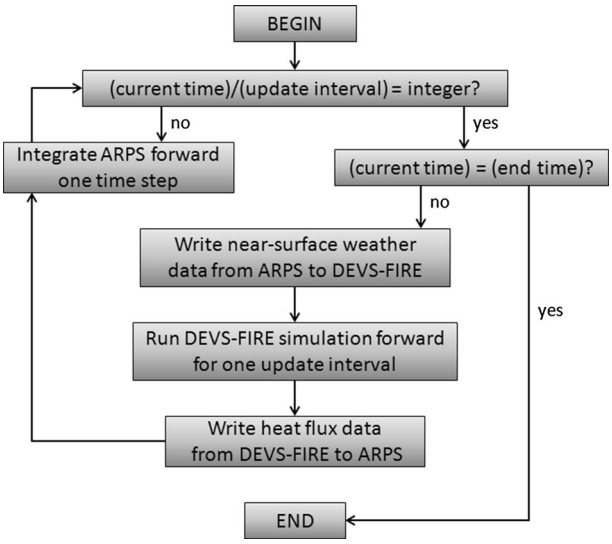

Fig. 4 Time integration algorithm for ARPS/DEVS-FIRE coupled model

spatially averages the heat flux data, maps the results onto its own grid, and integrates forward to the next update time. The new weather conditions are then interpolated to the DEVS-FIRE grid, the spread rates and neighbor cell ignition times are updated, and the process repeats.

The simulations shown here were assumed to represent fires that burned for some time prior to initialization. Therefore, the entire surface area of the each cell comprising the initial fire front was ignited immediately, in contrast to more gradual ignition methods used when model initialization and fire ignition are meant to be simultaneous (e.g., the "drip-torch" method detailed in Mandel et al. 2011). This approach neglected heat output from areas burned prior to the initial time; however, reliable data for the geographic extent and heat output of such regions at a given time is not generally available, and the *ad hoc* introduction of smolder regions into the initial conditions for DEVS-FIRE failed to substantially alter any of the results presented here.

4 Evaluation of the coupled model

4.1 Idealized coupled tests

The use of idealized tests to verify the coupled model has limitations, e.g., the lack of an analytical solution for the fire spread that can be used for quantitative verification. Nevertheless, such tests can qualitatively illustrate the model's ability to mimic theoretically expected behavior. Two aspects of coupled fire–atmosphere behavior are considered here: (1) the manner in which coupling leads to localized enhancement of fire spread and (2) the manner in which variations in background weather conditions, grid resolution, and amount of interpolation increase or diminish the impact of coupled phenomena.

As described in Clark et al. (1996), coupling the fire to the atmosphere produces a nonlinear feedback between the environmental winds and the fire spread through the

generation of vertical vorticity along the fire front. In brief, the intense heat from the fire generates a sharp atmospheric buoyancy gradient, which in turn induces horizontal vorticity that can be modified (through tilting and stretching associated with the fire plume) to strengthen the winds across the fire front. Thus, the fire spreads more rapidly, which increases the heat release, and the process repeats; one observed impact of this feedback is to produce parabolic "fingers" in the fire front. Clark et al. (1996) state that this process is contingent on a balance between the kinetic energy of the background atmosphere and the heat energy produced by the fire spread. When the kinetic energy of the wind across the fire front is large compared to the heat energy imparted to the lower atmosphere by the fire, the local wind theoretically should not be substantially affected because small residence time and/or comparatively weak heat flux convergence results in minimal heating of air parcels traversing the fire front. When the heat energy from the fire predominates, air parcels are subjected to intense heating and the potential for vigorous feedbacks exists.

However, Sullivan (2007) notes a lack of evidence for strong one-to-one correlation between this kinetic-thermal energy balance and intense feedback-related phenomena during controlled experimental burns. Those results suggest that other factors may be crucial to nonlinear intensification. Therefore, examination of the ARPS/DEVS-FIRE model's ability to handle coupling realistically cannot simply rely on a quantitative assessment of the change in burn area due to coupling. To provide some quantitative basis for evaluating model performance, idealized 30-min tests were performed in which an initial fire front 2 km long and 90 m deep was centered on the east–west midline of a DEVS-FIRE domain extending 18 km east-to-west and 3.6 km north-to-south under a uniform background westerly wind, with firebreaks placed immediately upstream of the initial fire front. The midline therefore denotes a theoretical line of symmetry; asymmetry across this line (as observed in other coupled models, e.g., CAWFE in Clark et al. 2004) can provide one measure of accumulated model truncation error.

In order to prevent the fire from reaching the ARPS lateral boundaries, a domain 19 km in length and 4 km in width was specified for ARPS and the DEVS-FIRE grid was centered within the ARPS grid. DEVS-FIRE grid spacing was selected with the goals of (1) collocating the centers of ARPS and DEVS-FIRE grid cells wherever possible and (2) collocating the centers of cells in DEVS-FIRE grids with different resolutions wherever possible. Furthermore, this experiment was designed to test both the impact of changing the DEVS-FIRE resolution and the impact of increasing the amount of interpolation and spatial averaging being done. Therefore, the ARPS horizontal resolution was set to 90 m and DEVS-FIRE grid resolutions of 10, 30, and 90 m were employed. 4 m vertical resolution was selected for the ARPS grid near the ground, stretched to an average of 100 m aloft to afford ample domain depth to contain the plumes produced by the fire. Since the computational locations for the horizontal wind components ("U" and "V" in Fig. 3) are midway between the upper and lower faces of the Arakawa-C cell, this selection placed the "U" and "V" locations for the second vertical grid level at the 6 m elevation required for the DEVS-FIRE wind input, thereby removing any need for vertical interpolation in the coupling algorithm.

For simplicity, the possibility of additional feedbacks stemming from preexisting environmental shear (such as those described in Kiefer et al. 2009) was deemed undesirable; therefore, each simulation used a neutrally stratified base-state atmosphere with a uniform westerly wind of 3 or 12 m s^{-1} for the initial and boundary conditions in ARPS. A completely flat field of tall, fully cured dead grass (fuel category 3 from Anderson 1982 with a specified moisture content of 3 %) was mapped to the DEVS-FIRE grid. To evaluate the impact of coupling the models, pairs of simulations were run for each combination of

Table 2 Comparison of coupled (C) versus uncoupled (UC) burn areas from idealized simulations at $t = 1{,}800$ s

DEVS-FIRE grid resolution (m)	Background wind speed (m s^{-1})	UC burn area (km^2)	Burn area difference (C–UC, km^2)	Normalized difference (%)	Accumulated asymmetry in coupled simulation (%)
10	3	2.07	3.71	179.2	0.22
30	3	2.01	3.61	179.9	0.79
90	3	1.96	1.39	71.1	2.95
10	12	10.91	0.63	5.8	0.16
30	12	10.77	0.97	9.0	0.54
90	12	10.48	0.73	7.0	0.86

DEVS-FIRE resolution and initial wind speed (6 in all; see Table 2). Along with the coupled simulation, an uncoupled simulation was performed in which ARPS was allowed to update DEVS-FIRE but not vice versa; this was done to account for any impact of DEVS-FIRE grid resolution on burn area, as well as any non-fire-related disturbances in ARPS, e.g., due to surface friction.

For quantitative evaluation, the difference in burn area between the coupled and uncoupled simulation in each pair was calculated, along with the asymmetry of the coupled model solution. The asymmetry is defined here as the normalized RMS difference between the heat flux produced by cells on the north side of the line of symmetry and their mirror-image counterparts on the south side at each update time, averaged over all update times. Furthermore, a qualitative evaluation of the "realism" of each fire front shape was performed in light of the results obtained by vector-based coupled models in similar tests (e.g., WRF-FIRE in Mandel et al. 2011, HIGRAD/FIRETEC in Linn and Cunningham 2005).

The quantitative results are listed in Table 2, while the outlines of the 30-min burn areas are plotted in Fig. 5. The impact of model coupling on burn area was apparent in all cases, although it was substantially less in the simulations with higher wind speeds. Furthermore, it is apparent that increasing DEVS-FIRE grid spacing artificially reduced the uncoupled spread rate, with a greater impact observed at the higher wind speed. There also appears to be a sharp decline in coupled model performance from 30 to 90 m resolution at the slower wind speed, in terms of the impact of coupling on burn area as well as the model error implied by the asymmetry (At the higher wind speed, the impact of DEVS-FIRE resolution on coupled burn area is unclear, although coarser resolution still produced more asymmetry).

Figure 5 demonstrates that the impacts go beyond the quantitative results. It is clear that the fire front in the uncoupled DEVS-FIRE model developed an unrealistically flat shape. Coupling with the ARPS model introduced local variations that produced more realistic curves. Furthermore, as with similar tests using other coupled models, the degree to which these shapes conform with the "classic" parabolic or conical shape (e.g., as detailed in Clark et al. 1996) varies based on wind speed, ignition line length, and DEVS-FIRE resolution. At the slower wind speed, the development of a parabolic fire front was disrupted in the 10 and 30 m simulations by the development of persistent vortices along the flanks which propagated slowly toward the center of the fire front; the resulting counterflow in the center produced a concave fire front shape similar to that shown in Figure 2 of Linn and Cunningham (2005) and Figure 8 of Mandel et al. (2011). In keeping with results from HIGRAD/FIRETEC in Linn and Cunningham (2005), a subsequent 10 m resolution

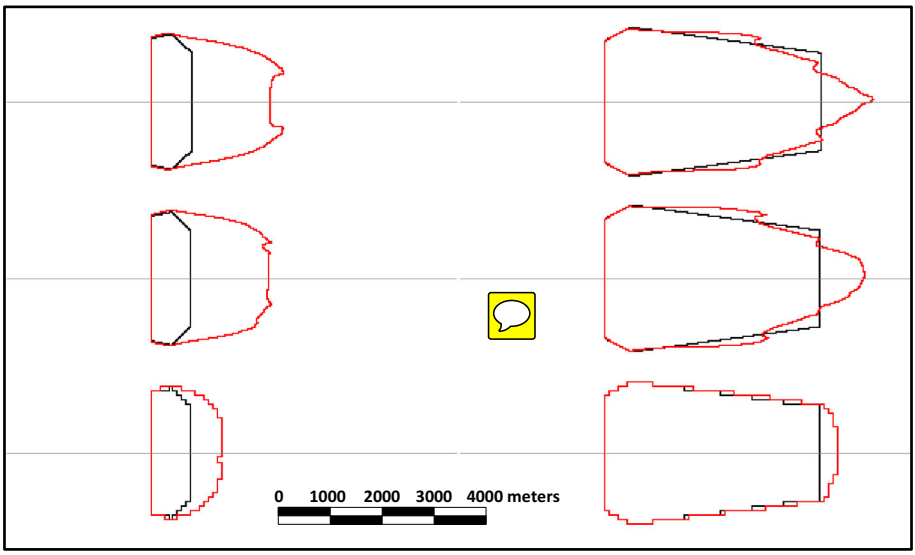

Fig. 5 Burn areas at $t = 1{,}800$ s for idealized uncoupled (*black*) and coupled (*red*) simulations for initial surface winds of 3 m s^{-1} (*left*) and 12 m s^{-1} (*right*) and DEVS-FIRE grid resolutions of 10 m (*top*), 30 m (*middle*), and 90 m (*bottom*). *Thin lines* denote east–west lines of symmetry, and the images are zoomed to the burn areas, located in the western halves of the DEVS-FIRE grids

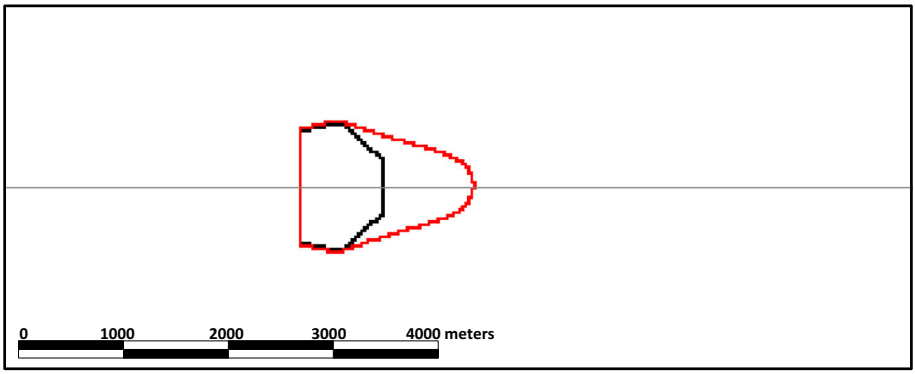

Fig. 6 Same as Fig. 5, but for a 0.5 km ignition line with a background wind speed of 3 m s^{-1} and a DEVS-FIRE resolution of 10 m

test in which the ignition line length was reduced to 0.5 km produced a more familiar parabolic shape as shown in Fig. 6, demonstrating a dependence on ignition line length as well.

At the faster wind speed, the vortices quickly moved away from the flanks and were not as much of a factor. This allowed the fire front to assume a more parabolic shape in the 10 and 30 m simulations as shown on the right side of Fig. 5. As in the quantitative analysis, it is clear that the 10 and 30 m results are comparable, while the coupling in the 90 m simulation appears unrealistically muted. Hence, these initial experiments suggest that the

use of DEVS-FIRE grid resolutions up to 30 m may produce reasonable results, while the use of a coarser resolution appears suspect.

4.2 The Moore Branch Fire: September 6, 2000

Along with the idealized simulations, the September 2000 Moore Branch Fire was selected as a case study for testing the performance of the coupled model in a situation with real fuel and weather data by comparing the simulation results with the actual observed burn area. This case was chosen due to the availability of representative, high-resolution fuel and terrain survey data from the Texas Forest Service, along with indications of nonlinear fire behavior as summarized below.

4.2.1 Event synopsis

A persistent region of high atmospheric pressure produced several consecutive days with high temperatures exceeding 38 °C (100 °F), extremely low daytime relative humidity, and patchy dry thunderstorm activity throughout southeast Texas in early September, 2000. Around 3:00 p.m. on September 1, crews responded to a wildland fire northeast of Newton. The blaze initially spread slowly through gently rolling terrain (with ground slope generally well under 10°; see Fig. 7) and appeared to be under control by September 3.

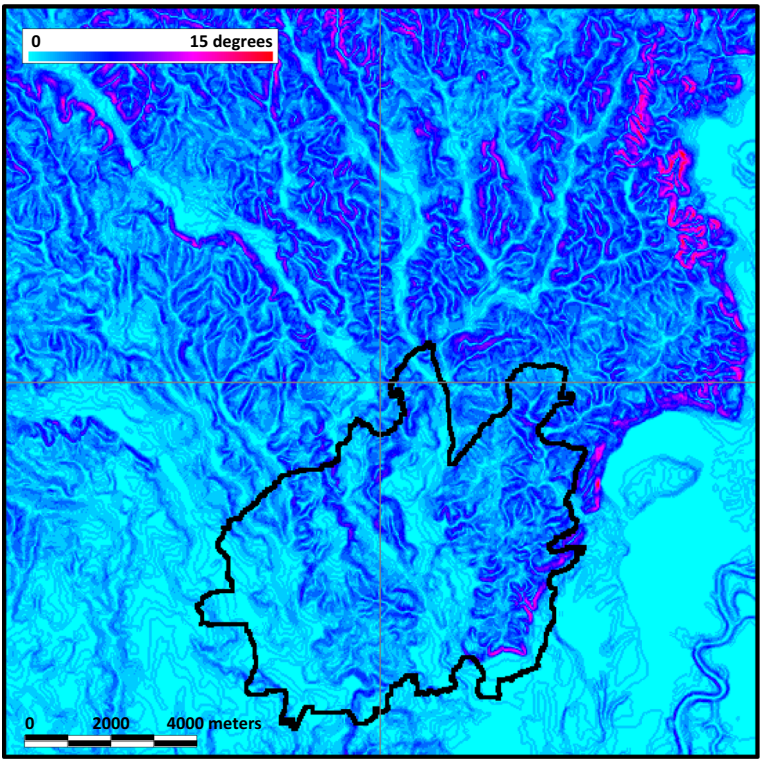

Fig. 7 Ground slope in the vicinity of the Moore Branch Fire; the *black outline* marks the area burned on Day 5

However, fire behavior became "extreme" the following day and completely unmanageable on September 5. In all, the fire burned more than 16,000 acres. (Bean 2000)

Evaluation of the causes for the fire spread on September 5 (hereafter "Day 5") is complicated by a lack of in situ weather data with good temporal resolution in close proximity to the burn area. At the time of the event, the nearest hourly weather observation station was located in Lake Charles, LA, over 50 miles away and separated from the fire site by complex, densely wooded terrain. However, a daily summary detailing the high and low temperatures, minimum relative humidity, maximum wind speed, and wind direction at noon was obtained from Kirbyville, located roughly 16 miles south-southwest of the fire. Those observations indicated a maximum daytime wind speed of 9.9 m s^{-1}, which was deemed to be the best available in situ measurement approximating conditions in the vicinity of the fire. In light of the discussion and idealized tests in the previous section, this wind speed suggests the possibility of coupled atmosphere–fire behavior playing a substantial role in the extreme fire behavior on Day 5.

4.2.2 Experimental procedure

Weather data scarcity complicated the preparation of the coupled model prior to initialization. 32-km reanalysis data from the National Center for Environmental Prediction indicate that the local wind speed and direction varied widely over the course of Day 5 (see Table 3). The Kirbyville observations were therefore insufficient to establish suitable initial and boundary conditions for the weather model. Furthermore, verification of the fire model results at regular intervals is not possible since observations establishing a "true" fire front location are only available for the beginning and end of the day.

Along with their comparatively coarse resolution, the reanalysis data are only available at 3-h intervals. In order to obtain background states more suited to the spatial and temporal resolutions of the coupled model, the reanalysis data were progressively downscaled using one-way grid nesting. The initial (12:00 a.m. September 5) data were interpolated to a smaller "intermediate" ARPS domain encompassing the Day 4 and Day 5 burn areas; this domain had a 2 km horizontal resolution and a vertical resolution of 4 m at the surface stretching to an average of 100 m aloft (similar to the grids used for the idealized tests) in order to capture vertical turbulent mixing of momentum in the boundary layer for transfer to an even finer-scale coupled grid. The background state was integrated forward 24 h using interpolated reanalysis data at later times for the boundary conditions. The results were interpolated at hourly intervals to smaller (18 km by 18 km) coupled ARPS domains

Table 3 Background weather conditions in the vicinity of the Moore Branch Fire on September 5, interpolated from NCEP reanalysis data

Time (CDT)	Wind speed (m s^{-1})	Wind direction (deg N)
12:00 a.m.	0.188	105
3:00 a.m.	1.835	22
6:00 a.m.	2.135	29
9:00 a.m.	5.569	42
12:00 p.m.	6.908	48
3:00 p.m.	4.775	49
6:00 p.m.	1.386	9
9:00 p.m.	2.480	16
12:00 a.m.	4.829	43

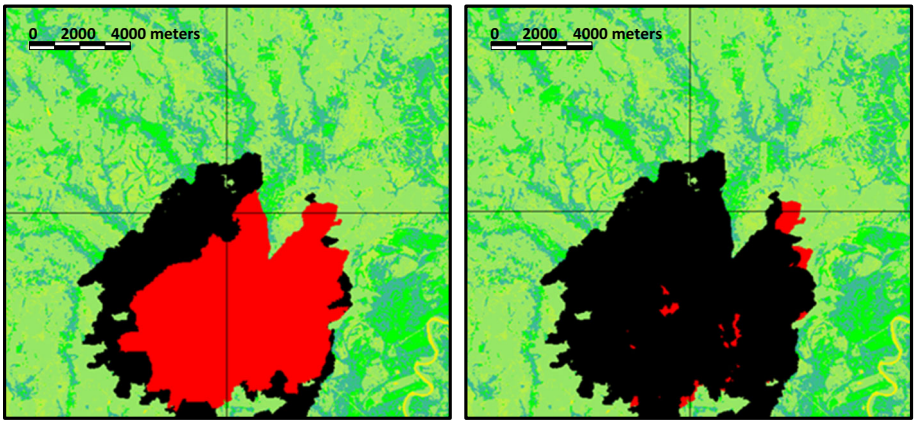

Fig. 8 Moore Branch Fire Day 5 actual burn area (*red*) and burn area predicted by DEVS-FIRE using weather observations from Kirbyville (*black*). The actual burn area is overlaid at *left* and underlaid at *right* to illustrate the relationships between the burn areas

at identical vertical resolution and 60, 150, 300, and 1,200 m horizontal resolution for use as initial and boundary conditions for the coupled simulations. For DEVS-FIRE, Texas Forest Service field data were used to construct a fuel and terrain grid at 30 m resolution that encompassed the Day 4 and Day 5 burn areas while falling entirely within the ARPS domain. The initial Day 5 fire front position (obtained from Texas Forest Service GIS data) was then defined on the DEVS-FIRE grid as a series of ignition point coordinates. (Since the fire had spread for several days prior to the initialization time of the model, artificial firebreaks were placed immediately behind the ignition line as a quick method of preventing spurious propagation over locations that had already burned on Day 4.)

To test the efficacy of the coupled model, several 24-h simulations were performed using all or part of this framework. First, a trial simulation was performed using only the DEVS-FIRE grid and the maximum wind speed and corresponding direction from the Kirbyville observations (wind speed 9.9 m s^{-1}, wind direction 33° from true north, both held constant for the full 24 h of simulation). Next, an uncoupled simulation (at 60 m resolution) and four coupled simulations (one each at 60, 150, 300, and 1,200 m resolution) were performed using the reanalysis data for initial and boundary conditions as described above (It should be noted here that an additional test included a 30-min initial period in which the fire front position and intensity were held constant in an effort to adjust the initial ARPS conditions to the presence of the fire before the fully coupled simulation began; however, the results did not differ substantially from those of the other coupled tests. Therefore, no further efforts to "spin up" ARPS were included in this work). Finally, simple visual and statistical verification of the results was performed by comparing the simulated burn area from each simulation with the actual burn area as reported by the Texas Forest Service.

4.2.3 Results and discussion

The results are illustrated in Figs. 8, 9 and 10. Figure 8 shows overprediction of fire spread in the trial simulation using the Kirbyville data, particularly to the west and south. However, even though the use of a single meteorological data point is a terribly simplistic approach, greatly overestimating the wind speed for most of the day and accounting for

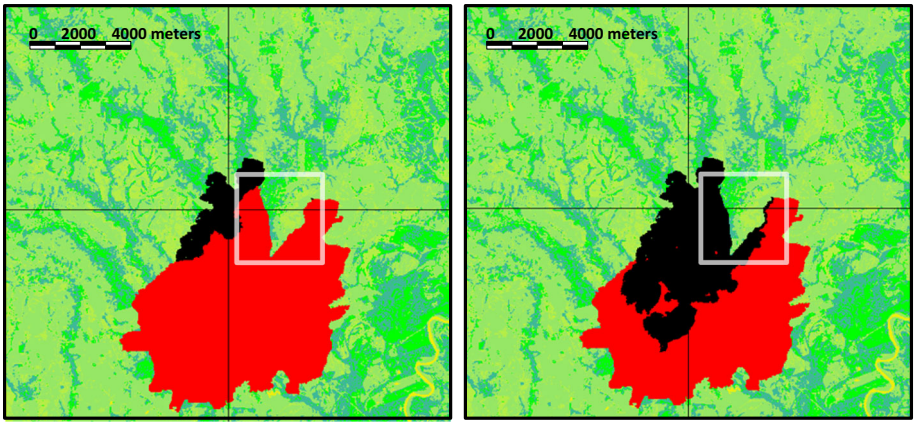

Fig. 9 Same as Fig. 8, but for results from the uncoupled ARPS/DEVS-FIRE simulation using large-scale weather reanalysis data. *White boxes* indicate the zoomed area plotted in Fig. 11

none of the variation in wind speed and direction indicated in Table 3, the fire spread from this test was surprisingly close to the actual Day 5 burn area. The fact that a clear overestimate of average background wind speed did not produce a corresponding overprediction for the Day 5 burn area suggests that the fire spread may have been substantially increased by processes that the background weather conditions do not adequately reflect.

This possibility is confirmed in Fig. 9, which compares the actual burn area to the burn area predicted by the uncoupled simulation. Except for minor modifications of the wind field due to higher-resolution treatment of the effects of surface friction and other interactions between the atmosphere and the terrain, the weather conditions in this simulation are largely interpolations of the reanalysis data and closely follow the conditions charted in Table 3. As a result, there is a clear underprediction of the fire spread, particularly in the eastern half of the burn area where the northeasterly background wind is roughly parallel to the initial fire front. Clearly, a localized wind adjustment with a stronger component normal to the eastern half of the fire front is needed to improve accuracy.

As shown in Fig. 11, coupling ARPS with DEVS-FIRE produces such an adjustment, leading to a much stronger southeasterly component in the local wind field near the eastern half of the fire front. Consequently, as shown in Fig. 10, the coupled ARPS/DEVS-FIRE simulations are far superior to the uncoupled simulation. In addition to generally increasing the spread rate by locally enhancing surface winds near the fire, the coupled simulations produce a much more accurate spread in directions perpendicular to the background wind. When compared to the results from the Kirbyville simulation, the overprediction of spread to the west and south is reduced while the general dimensions of the burn area are preserved.

Surprisingly, Fig. 10 also shows no substantial benefit from increasing the ARPS horizontal resolution beyond 300 m in this case. While coarse-grid artifacts (e.g., failure to resolve the initial fire front shape, which is only about 2 km from end to end) reduce the quality of 1,200 m simulation considerably, the 60, 150, and 300 m results are all quite similar. (No importance is currently assigned to the fact that the 300 m results actually improve slightly on the 60 and 150 m results due to both the marginal degree of improvement and the small sample afforded by a single case study.) While the 24-h 60-m test required 72 h to complete and was therefore much too slow to be of any hypothetical predictive use, the 300 m test completed in roughly 8 h (for a wall clock ratio of

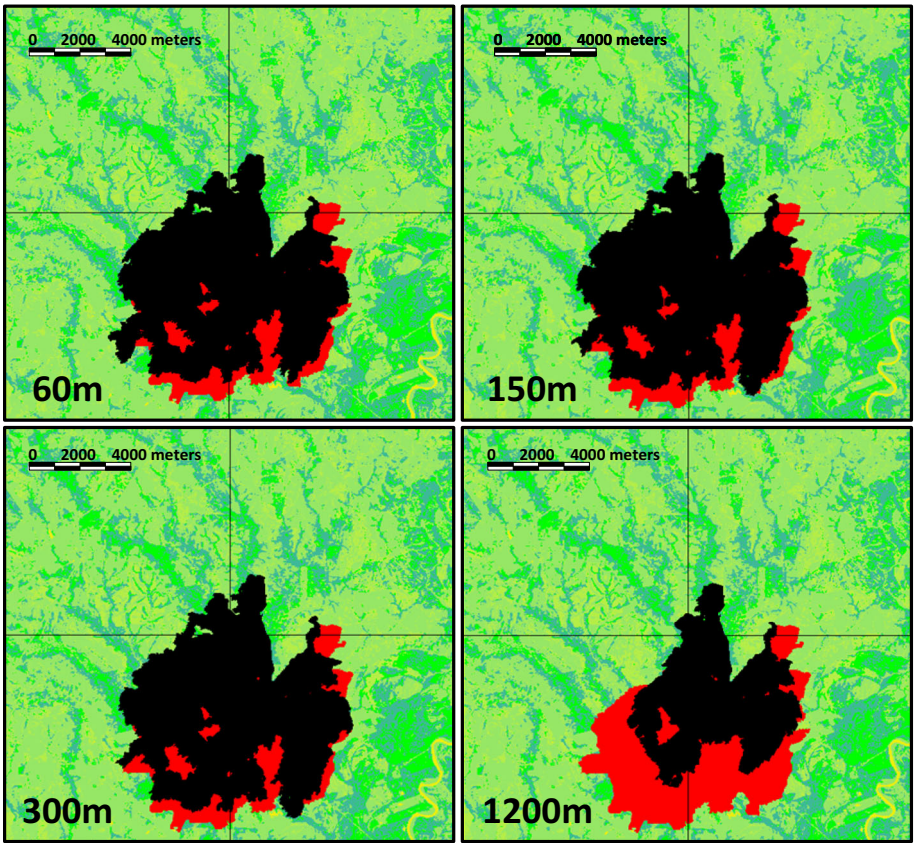

Fig. 10 Same as Fig. 9, but for results from the coupled ARPS/DEVS-FIRE simulations at 60 m (*upper left*), 150 m (*upper right*), 300 m (*lower left*), and 1,200 m (*lower right*) ARPS resolution

approximately 3). It must be noted that this is slower (by a factor of two) than the speed reported for WRF-FIRE at 400 m resolution in Mandel et al. (2011); however, when one factors in the current lack of optimization in both the code (with DEVS-FIRE running serially) and the coupling algorithm (with both models running separately and exchanging information externally), this is an encouraging result.

To confirm the visual analysis, the probability of detection (POD), false alarm rate (FAR), and Heidke Skill Score (HSS) were calculated for each simulation. These metrics were obtained by assigning each cell a value of "burned" or "unburned" at the end of Day 5 and counting the number of hits (both the observed and simulated cell burned), misses (the observed cell burned but the simulated cell did not), false alarms (the simulated cell burned but the observed cell did not), and true negatives (neither the observed nor the simulated cell burned). Denoting the number of hits as H, the number of misses as M, the number of false alarms as F, and the number of true negatives as N, the formulas for the metrics are as follows:

$$\mathrm{POD} = \frac{H}{H + M}$$

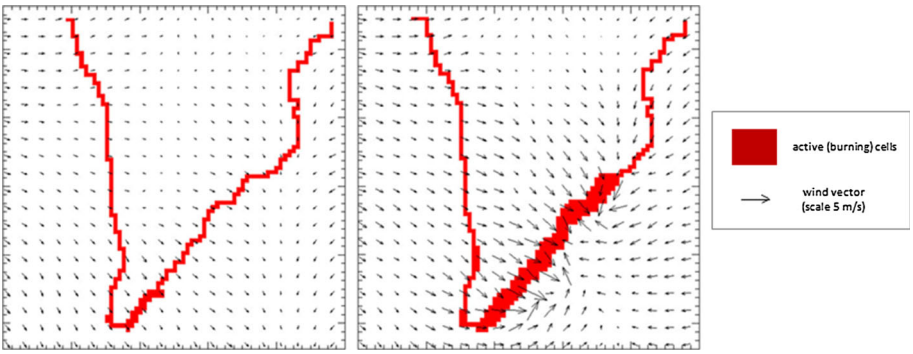

Fig. 11 Comparison between uncoupled (*left*) and 60 m coupled results (*right*) at $t = 40$ min for the Moore Branch Fire case. *Arrows* indicate near-surface horizontal wind speed and direction in the region indicated by the *white boxes* in Figs. 9 and 10

$$\mathrm{FAR} = \frac{F}{F+N}$$

$$\mathrm{HSS} = \frac{H+N-E}{H+M+F+N-E} \quad \text{where} \quad E = \frac{(H+M)(H+F)+(M+N)(F+N)}{(H+M+F+N)}$$

HSS was chosen as a skill metric because the parameter E accounts for correct forecasts obtained purely by chance. Also, to avoid contaminating the metrics with an inflated value for N, the northern 1/3rd of each domain was ignored since it was well outside the burn area in all cases. Table 4 lists the scores obtained after this adjustment was applied. While the Kirbyville simulation has the highest POD (unsurprising, given the large predicted burn area), the coupled simulations have a much lower FAR and the highest overall skill, outperforming the uncoupled simulation by a substantial margin (Again, reducing the ARPS resolution from 60 to 150 or 300 m actually improved the forecast slightly). When considered in conjunction with the unrealistic method used for the Kirbyville simulation (i.e., constant wind for the entire period based on a single measurement taken well after initialization), this analysis attests to the superiority of the coupled model in this case.

5 Future work

The foregoing coupled ARPS/DEVS-FIRE results are promising, demonstrating both reasonable behavior in idealized tests and improved forecast quality when compared to

Table 4 Statistical verification of ARPS/DEVS-FIRE simulations for Day 5 of the Moore Branch Fire

Simulation	POD	FAR	HSS
Kirbyville (constant)	0.951	0.202	0.626
Uncoupled	0.316	0.037	0.345
60 m coupled	0.805	0.093	0.689
150 m coupled	0.814	0.089	0.703
300 m coupled	0.816	0.087	0.708
1,200 m coupled	0.522	0.021	0.582

uncoupled methods for a particular wildland fire case. However, a good deal of work remains before the model can be fully validated as a forecast tool. For example, while the uncoupled ARPS model has been validated at LES resolutions under typical atmospheric conditions, its response to extreme surface fluxes (e.g., the structure and intensity of developing plumes) has not been quantitatively evaluated with reference to observed atmospheric conditions over wildland fires. The next step in our research is to perform and present simulations of the FIREFLUX experiment (Clements et al. 2007) in which in situ vertical profiles of temperature, moisture, and three-dimensional wind were acquired at high temporal resolution over an experimental burn in a well-sampled fuel bed on flat terrain. The observational data from this experiment have been used to validate atmospheric response as well as small-scale rate of spread in other coupled models (e.g., WRF-FIRE in Kochanski et al. 2013).

The current coupled model framework is not sufficiently optimized to enable run times comparable to those demonstrated by existing models like WRF-FIRE. One area of difficulty lies in the fact that the models currently run separately and exchange data externally; since the speed of external I/O on the supercomputing clusters used for this work varies based on user load, it is not possible to determine a reliable wall clock ratio when operating in this manner. The computational expense associated with the external I/O also heavily influenced the selection of the time interval used for updating the coupled model state; while the use of discrete event specification avoids the time step constraints faced by many other fire models (e.g., FARSITE), and the spatial averaging inherent in operating ARPS and DEVS-FIRE at different resolutions naturally smoothes the impact of larger shifts in fire front location from one update time to the next, the update interval should still be small in order to minimize the truncation error associated with nonlinear atmospheric response. Ideally, ARPS and DEVS-FIRE would update one another continuously; however, in the current non-optimized state, this was too costly, particularly for the Moore Branch simulations. Therefore, an interval of 60 s was selected as a more tractable value that also appeared to capture the main feedbacks at the operating resolution of ARPS. With the reasonable results of these initial tests, future efforts are focused on making the framework more suitable for operational use (e.g., enabling the models to run in tandem to remove the external I/O costs and developing a grid-nesting algorithm in DEVS-FIRE to distribute the interpolation and averaging costs more effectively).

Furthermore, questions have been raised regarding the representativeness of the CA-based, elliptical approach used to calculate the fire spread in different directions, particularly when used in conjunction with an atmospheric model. This method was selected for the current coupled framework because it is intended to approximate the effects of subgrid-scale processes (i.e., those that cannot be explicitly resolved by the model) on fire spread in order to provide more realistic fire front shapes than would result from only using a single spread rate and direction dictated by the background weather, fuel, and terrain. However, previous work (e.g., French et al. 1990; Trunfio et al. 2011) has illustrated an increased potential for distortion of the fire shape due to the limited degrees of freedom afforded to the spread. While the tests shown here do not appear to have been severely impacted by such distortion, further exploration of the merits of this approach is clearly needed, and further improvements (e.g., increased spread direction degrees of freedom, exploration of parameterizations other than the elliptical approximation) will likely be required.

Finally, operating DEVS-FIRE at coarser resolution produces increasingly discontinuous fire behavior, while reducing the grid spacing to a discretization level approaching the behavior of more continuous methods (e.g., the integral method detailed in Mandel

et al. 2011) incurs greater computational cost. It would therefore be valuable to have a greater understanding of "optimum" operating resolutions. This is particularly crucial for the weather model, which is the most expensive component; the results presented here suggest that operating ARPS at a resolution on the order of a few hundred meters *may* be sufficient to capture the important feedbacks in many cases and would reduce computation time substantially. However, the robustness of this finding is clearly not established, and additional test cases are needed to provide context to the results obtained in this study.

Acknowledgments This work was accomplished under NSF Grants CNS-0941432, CNS-0941491, and CNS-0940134 and made extensive use of the Gordon, Sooner, and Kraken supercomputing clusters. The authors wish to thank the San Diego Supercomputing Center, the OU Supercomputing Center for Education and Research at the University of Oklahoma, the National Institute for Computational Sciences at the University of Tennessee, and the Oak Ridge National Laboratory for making those resources available and providing technical support. We also express our appreciation to Thomas Spencer and Curt Stripling of the US Texas Forest Service for providing the GIS data related to the Moore Branch Fire, the National Climatic Data Center for providing the necessary background weather data for our tests, and the reviewers whose feedback greatly improved the quality of this manuscript.

References

Achtemeier GL (2003) "Rabbit Rules": an application of Stephen Wolfram's "New Kind of Science" to fire spread modelling. In: Fifth symposium on fire and forest meteorology, 16–20 Nov 2003. American Meteorological Society, Orlando, Florida

Achtemeier GL (2013) Field validation of a free-agent cellular automata model of fire spread with fire–atmosphere coupling. Int J Wildland Fire 22:148–156

Albini FA, Reinhardt ED (1995) Modeling ignition and burning rate of large woody natural fuels. Int J Wildland Fire 5(2):81–91

Anderson H (1982) USDA Forest Service, Intermountain Forest and Range Experiment Station. General Technical Report INT-122

Arakawa A, Lamb VR (1977) Computational design of the basic dynamical processes of the UCLA general circulation model. Methods Comput Phys 17:173–265

Bean O (2000) Moore Branch Fire. Texas Forest Service, Texas A&M University System, College Station

Byram GM (1959) Forest fire behavior. In: Davis KP (ed) Forest fires: control and use. McGraw-Hill, New York, pp 90–123

Chow FK, Weigel AP, Street RL, Rotach MW, Xue M (2006) High-resolution large-eddy simulations of flow in a steep alpine valley. Part I: methodology, verification, and sensitivity experiments. J Appl Meteorol Climatol 45:63–86

Clark TL, Jenkins MA, Coen JL, Packham DR (1996) A coupled atmosphere–fire model: role of the Convective Froude number and dynamic fingering at the fireline. Int J Wildland Fire 6:871–901

Clark TL, Coen JL, Latham D (2004) Description of a coupled atmosphere–fire model. Int J Wildland Fire 13:49–63

Clements CB, Zhong SY, Goodrick S, Li J, Potter BE, Bian XD, Charney JJ, Heilman WE, Perna R, Jang M, Lee D, Patel M, Street S, Aumann G (2007) Observing the dynamics of wildland grass fires: fireflux—a field validation experiment. Bull Am Meteorol Soc 88:1369–1382

Deardorff JW (1980) Stratocumulus-capped mixed layers derived from a three-dimensional model. Boundary Layer Meteorol 18:495–527

Filippi JB, Bosseur F, Pialat X, Santoni PA, Strada S, Mari C (2011) Simulation of coupled fire/atmosphere interaction with the MesoNH-ForeFire models. J Combust. doi:10.1155/2011/540390

Finney MA (1998) FARSITE: Fire area simulator-model development and evaluation. USDA Forest Service, Rocky Mountain Research paper RMRS, RP-4 Ogden, UT

French IA, Anderson DH, Catchpole EA (1990) Graphical simulation of bushfire spread. Math Comput Model 13:67–71

Green D, Gill A, Noble I (1983) Fire shapes and the adequacy of fire-spread models. Ecol Model 20(1):33–45

Gu F, Hu X, Ntaimo L (2008) Towards validation of DEVSFIRE wildfire simulation model. In: Proceedings of the 2008 high performance computing and simulation symposium, pp 355–361

Hu X, Ntaimo L (2009) Integrated simulation and optimization for wildfire containment. ACM Trans Model Comput Simul (TOMACS) 19(4): Article No. 19
Hu X, Sun Y (2007) Agent-based modeling and simulation of wildland fire suppression. In: Proceedings of the 2007 winter simulation conference, pp 1275–1283
Hu X, Sun Y, Ntaimo L (2012) DEVS-FIRE: design and application of formal discrete event wildfire spread and suppression models. Simulation 88(3):259–279
Karafyllidis I, Thanailakis A (1997) A model for predicting forest fire spreading using cellular automata. Ecol Model 99(1):87–97
Kiefer MT, Parker MD, Charney JJ (2009) Regimes of dry convection above wildfires: idealized numerical simulations and dimensional analysis. J Atmos Sci 66:806–836
Kochanski A, Jenkins M, Mandel J, Beezley J, Clements CB, Krueger S (2013) Evaluation of WRF-Sfire performance with field observations from the FireFlux experiment. Geosci Model Dev 6:1109–1126
Kolmogorov AN (1941) Dissipation of energy in isotropic turbulence. Dokl Akad Nauk SSSR 32(1):19–21
Kourtz P, O'Regan W (1971) A model for a small forest fire to simulate burned and burning areas for use in a detection model. For Sci 17(1):163–169
Linn RR, Cunningham P (2005) Numerical simulations of grass fires using a coupled atmosphere-fire model: basic fire behavior and dependence on wind speed. J Geophys Res 110:D13107. doi:10.1029/2004JD005597
Lopes A, Cruz M, Viegas D (2002) Firestation—an integrated software system for the numerical simulation of fire spread on complex topography. Environ Model Softw 17(3):269–285
Lundquist KA, Chow FK, Lundquist JK (2012) An immersed boundary method enabling large-eddy simulations of flow over complex terrain in the wrf model. Mon Weather Rev 140:3936–3955
Mandel J, Beezley JD, Kochanski AK (2011) Coupled atmosphere-wildland fire modeling with WRF 3.3 and SFIRE 2011. Geosci Model Dev 4(3):591–610
Moeng C (1984) A large-eddy-simulation model for the study of planetary boundary-layer turbulence. J Atmos Sci 41:2052–2062
Ntaimo L, Zeigler BP, Vasconcelos MJ, Khargharia B (2004) Forest fire spread and suppression in DEVS. Simulation 80(10):479–500
Ntaimo L, Hu X, Sun Y (2008) DEVS-FIRE: towards an integrated simulation environment for surface wildfire spread and containment. Simulation 84(4):137–155
Obukhov AM (1946) Turbulence in an atmosphere with a non-uniform temperature. Trudy Inst Theor Geofiz AN SSSR 1:95–155
Peterson S, Morais ME, Carlson JM, Dennison PE, Roberts DA, Moritz MA, Weise DR (2009) Using HFire for spatial modeling of fire in shrublands. USDA Forest Service, Pacific Southwest Research Station, Research Paper PSW-RP-259. Albany, CA
Rothermel RC (1972) A mathematical model for predicting fire spread in wildland fuels. USDA Forest Service research paper INT, 115. Ogden, Utah
Sharples JJ (2008) Review of formal methodologies for wind–slope correction of wildfire rate of spread. Int J Wildland Fire 17:179–193
Skamarock WC, Klemp JB, Dudhia J, Gill DO, Barker DM, Duda MG, Huang X, Wang W, Powers JG (2008) A description of the advanced research WRF Version 3. NCAR Technical Note NCAR/TN-475 + STR. http://www2.mmm.ucar.edu/wrf/users/docs/arw_v3.pdf. Accessed 5 Jan 2015
Sullivan AL (2007) Convective Froude number and Byram's energy criterion of Australian experimental grassland fires. Proc Combust Inst 31:2557–2564
Sullivan AL (2009) Wildland surface fire spread modeling, 1990–2007. 3: simulation and mathematical analogue models. Int J Wildland Fire 18:387–403
Trunfio GA, D'Ambrosio D, Rongo R, Spataro W, Di Gregorio S (2011) A new algorithm for simulating wildfire spread through cellular automata. ACM Trans Model Comput Simul 22:1–26
Vasconcelos M, Guertin D (1992) FIREMAP—simulation of fire growth with a geographic information system. Int J Wildland Fire 2(2):87–96
von Neumann J (1966) The theory of self-reproducing automata. University of Illinois Press, Urbana
Xue H, Hu X (2011) Estimation of new ignited fires using particle filters in wildfire spread simulation. In: 44th annual simulation symposium, Boston, MA, USA
Xue M, Droegemeier KK, Wong V (2000) The Advanced Regional Prediction System (ARPS)—a multi-scale nonhydrostatic atmospheric simulation and prediction tool. Part I: model dynamics and verification. Meteorol Atmos Phys 75:161–193
Xue M, Droegemeier KK, Wong V, Shapiro A, Brewster K, Carr F, Weber D, Liu Y, Wang D-H (2001) The Advanced Regional Prediction System (ARPS)—a multiscale nonhydrostatic atmospheric simulation and prediction tool. Part II: model physics and applications. Meteorol Atmos Phys 76:134–165

Xue H, Gu F, Hu X (2012a) Data assimilation using sequential monte carlo methods in wildfire spread simulation. ACM Trans Model Comput Simul (TOMACS) 22(4):1–25

Xue H, Hu X, Dahl N, Xue M (2012b) Post-frontal combustion heat modeling in DEVS-FIRE for coupled atmosphere-fire simulation. In: 2012 international conference on computational science, Omaha, Nebraska, USA

Zeigler BP, Kim TG, Praehofer H (2000) Theory of modeling and simulation. Academic Press, Orlando

Zhou B, Chow FK (2011) Large-eddy simulation of the stable boundary layer with explicit filtering and reconstruction turbulence modeling. J Atmos Sci 68:2142–2155

Zhou B, Chow FK (2013) Nighttime turbulent events in a steep valley: a nested large-eddy simulation study. J Atmos Sci 70:3262–3276

Zhou B, Chow FK (2014) Nested large-eddy simulations of the intermittently turbulent stable atmospheric boundary layer over real terrain. J Atmos Sci 71:1021–1039